HHS Public Access

Author manuscript

*Anal Chem*. Author manuscript; available in PMC 2024 July 22.

Published in final edited form as:

*Anal Chem*. 2024 March 05; 96(9): 3687–3697. doi:10.1021/acs.analchem.3c04176.

# Dominant Analytical Techniques in DNA Nanotechnology for Various Applications

**Kayla Neyra**,
Department of Chemistry, Case Western Reserve University, Cleveland, Ohio 44106, United States

**Heather R. Everson**,
Department of Chemistry, Case Western Reserve University, Cleveland, Ohio 44106, United States

**Divita Mathur**
Department of Chemistry, Case Western Reserve University, Cleveland, Ohio 44106, United States

## Abstract

DNA nanotechnology is rapidly gaining traction in numerous applications, each bearing varying degrees of tolerance to the quality and quantity necessary for viable nanostructure function. Despite the distinct objectives of each application, they are united in their reliance on essential analytical techniques, such as purification and characterization. This tutorial aims to guide the reader through the current state of DNA nanotechnology analytical chemistry, outlining important factors to consider when designing, assembling, purifying, and characterizing a DNA nanostructure for downstream applications.

## Graphical Abstract

**Corresponding Author**: **Divita Mathur** – *Department of Chemistry, Case Western Reserve University, Cleveland, Ohio 44106, United States;* dxm700@case.edu.

Author Contributions

The manuscript was written through contributions of all authors. All authors have given approval to the final version of the manuscript.

The authors declare no competing financial interest.

ASSOCIATED CONTENT

Supporting Information

The Supporting Information is available free of charge at https://pubs.acs.org/doi/10.1021/acs.analchem.3c04176.

Design principles in DNA nanotechnology, factors that impact DNA nanostructure self-assembly, and scalability of DNA nanostructures, (PDF)

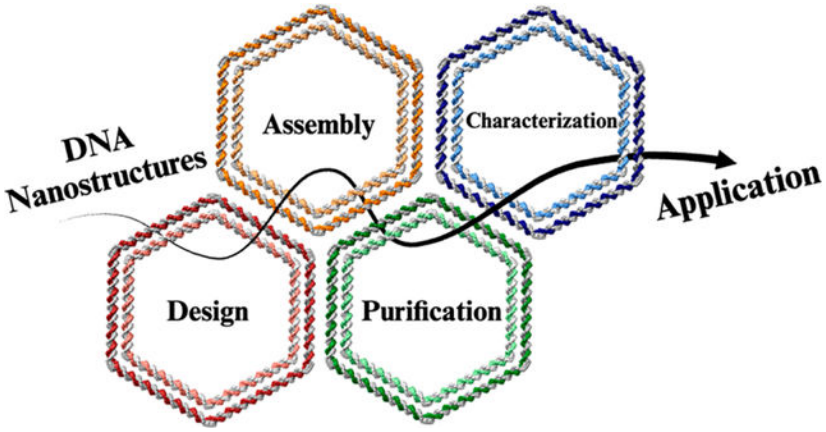


## INTRODUCTION

Deoxyribonucleic acid (DNA) is widely known for its role as the carrier of genetic material, but over the decades, the properties of this biopolymer have proven resourceful to create self-assembling nanostructures for bottom-up material synthesis. In utilizing the programmability and self-assembling properties of DNA, various nanostructures can be precisely designed with a defined shape, size, and surface functionality (Figure 1). As a biomolecule, DNA holds a significant advantage over other polymers and nanoparticles, as it offers a highly versatile, customizable, and biocompatible platform. Versatility means that practically any architecture or shape can be realized from DNA precursors by understanding and programming DNA's fundamental Watson–Crick–Franklin and Hoogsteen base pairing rules (Figure 2).[1–3] Customizability implies that a single strand of DNA oligonucleotide (ssDNA) can be chemically modified to attach other functional groups, nanoparticles, peptides, lipids, and fluorescent molecules with high efficiency.[4] In addition, biocompatibility, as in the ability of DNA nanostructures to coexist inside a mammalian body without untoward toxicity, is surprisingly high enough, even though the immune system is programmed to recognize and respond to foreign DNA.[5–7]

Because of these unique features, DNA nanostructures regularly appear in the areas of biomedicine, biomolecular engineering, nanofabrication, and nanotechnology now.[8,10] DNA nanostructures enable the precise and targeted delivery of therapeutic agents to specific cells or tissues.[11–13] In functionalization of these structures, the topology can be modified with targeted ligands or antibodies that enhance selectivity and reduce side effects of different therapies.[11,14] In the realm of bioimaging, the platform can be tagged with fluorescent dyes or other imaging agents that enable visualization and high-resolution imaging of biological structures.[15,16] DNA nanostructures have also been employed in molecular sensing applications, where they can be functionalized with specific receptors to detect and quantify target analytes such as proteins.[17,18] Additionally, DNA nanoplatforms augment photonic and nanoparticle plasmonic properties, enabling control over light–matter interactions.[19,20] DNA even has a place in the realm of computing and information storage; it serves as a promising medium due to the potential for parallel processing.[21,22]

These applications collectively demonstrate that DNA nanostructures are advancing various directions in basic science and technology.[23] However, the successful deployment of DNA nanostructures in all applications heavily relies upon their respective purification and characterization assays, which are the backbone of optimal performance. DNA-based nanostructures reside at the intersection of biomolecules and nanoparticles, which enables borrowing analytical techniques from both materials science and molecular biology to purify and characterize them. In this article, we highlight recent advances in the role of analytical chemistry toward application-specific purification and characterization of DNA nanostructures. To motivate the discussion, we first briefly summarize the designing and assembly of DNA nanostructures (see the Supporting Information) and then shed light on which analytical techniques have gained traction to achieve application-specific high-quality nanostructures.

## PURIFICATION OF DNA NANOSTRUCTURES

By design, DNA origami nanostructure assembly entails combining the scaffold strand with an excess of staple strands, typically 3- to 10-fold excess. DNA tile, brick, and staple assembly paradigms use equimolar amounts of the constituent strands. Even under ideal assembly conditions that result in near 95% folding efficiency, the annealing process will, thus, leave behind unincorporated strands in the solution. DNA origami structures form with 80–90% efficiency while tile assembly formation efficiency is variable with an average efficiency of 40%.[24] DNA nanostructures are typically created for hosting proteins, inorganic nanoparticles, and fluorescent molecules site-specifically. This often entails combining the nanostructures with an excess of these other molecules or DNA oligomers that are chemically modified with functional groups. Thus, when a broad assortment of biomolecules is required for product formation, the impurities or undesired byproducts mirror the assortment and make purification a challenge. Cumulatively, examples of unwanted residues would be unreacted DNA strands (excess staples), misfolded nanostructures, residual enzymes, or nanoparticles that may be present, depending on the application of the structure. These impurities can interfere with the subsequent functionalization and functionality of DNA nanostructures. The choice of the most suitable purification method is based on a balance of quantitative and qualitative factors: yield of structure recovered versus type of residual impurity. We discuss several purification techniques and their roles in purifying DNA nanostructures in an application-specific manner. There are several common purification techniques that are diverse in the sense that they can be applied to all disciplines of DNA nanotechnology (Table 1). The premise for each of these methodologies and their advantages/disadvantages are outlined below.

Agarose gel electrophoresis (AGE) separates molecular components based on their charge-to-mass ratio. That ratio for DNA is linearly correlated to its length, so AGE can separate different DNA species in a size-dependent manner. Neutral analogues of DNA such as peptide nucleic acid (PNA) have no migration on their own unless combined with intercalating stains.[25] Shorter DNA fragments will travel through the gel-matrix under an electric field at a faster rate than larger ones, and their position in the matrix can be visualized as fluorescent bands via intercalating stains to determine the size of each separate constituent. For DNA constructs, AGE often serves as the first line of characterization of

formation by measuring the fluorescent intensity of the gel band corresponding to the DNA structure (usually a high molecular weight band) as a fraction of the intensity of the band from the DNA scaffold alone. The DNA construct could then be purified by excising the band and using cellulose columns to separate the DNA structure out of the gel. Typically, AGE-purified DNA structures are highly pure and reliably free of residual short oligomers, proteins, nanoparticles, and higher-order aggregates. However, average yields observed in known work are 20–40% for both unmodified and functionalized structures.[26,27]

AGE will provide insight into whether a DNA nanostructure has formed, but it cannot give any details at molecular level resolution. Formation can be evaluated not only by the intensity of band migration but also by the distance. As shown in Figure S2A, a “magnesium screening” to evaluate the optimal salt concentration needed for DNA nanostructure assembly is based on gel migration. Even for preliminary assessment on the formation efficiency, however, some key variables can critically affect the rigor of measurements, namely, the DNA/gel staining method for visualization, the concentration of salt added during agarose gel preparation (which could be different from the salt used during DNA nanostructure assembly), and the salt concentration in the loaded samples themselves. Staining the gel using ethidium bromide has slowly been phased out for noncarcinogenic alternatives such as GelRed and SYBR dyes. These intercalators are positively charged and, when added before the AGE process is run, can affect the migration and spacing of constituent samples. Poststaining the gel after the AGE is complete mitigates stain-dependent variability in migration.[28] Quantity of salt in the gel buffer or gel itself can affect DNA migration.[29] AGE has become the first order of characterization of DNA nanostructures for all applications as well and is therefore classified as a technique of good quality (accurate preliminary information regarding structure formation) but of poor quantity (extremely low recovery yield and low scalability). Moreover, as can be seen, AGE serves simultaneously as a purification and characterization tool.

Ultrafiltration techniques enable the removal of smaller contaminants that may be present in solution while retaining larger DNA origami structures. Size-excluding filter columns are commercially available for different molecular weight cutoffs (MWCOs). Typically, DNA origami nanostructures are 4–8 MDa large while the impurities are 1 order of magnitude, if not smaller, in size, making filtration appealing. DNA nanostructures purified via ultrafiltration are best used in applications that are not affected by any larger or aggregated byproducts since those will be retained. However, for samples with smaller impurities, ultrafiltration is a reliable option that will aid in purifying the nanostructures relatively quickly. As an example, Shaw et al. quantified the purification efficiency of nanostructures functionalized by either fluorescent dyes (Alexa Fluor 488) or proteins (IgG/Ferritin).[26] In the dye-modified construct, ultrafiltration was used to give a resulting yield of around 82%, but in the two protein constructs, the recovery was unable to be measured due to the limited separation between the residual proteins and nanostructure itself; for reference, Alexa 488 is about 45 kDa, and IgG and Ferritin have molecular weights of 150 and 480 kDa, respectively.[26] Additionally, this method is ideal for small working volumes, as the filter columns are only able to hold a maximum of 500 $\mu$L at a time.[30] There are 15 mL alternatives available, but the loss in good product is correlated with the surface area of the cellulose membrane within the column, thereby giving poorer performance on

scale-up. In regards to design specification, this method is the least effective for rod-like constructs because they are able to pass through the filter unit if oriented favorably, leading to significant sample loss and, in turn, low yield.[30] To combat low yield, this purification technique demands a multifold excess starting material. Some structures require more than the recommended number of rinse steps to remove excess staples; such details are often missing from the published protocols. Ultrafiltration can therefore be classified as a technique with mediocre quality (cannot separate higher MW byproducts) and low quantity (considerable loss of desired product).

Over the past few years, DNA precipitating agents such as polyethylene glycol (PEG)[31] and ethanol[32] are increasingly being applied for purifying DNA nanostructures from the smaller residual oligonucleotides. Here, the precipitating agent is used to selectively precipitate DNA origami constructs by aggregating structures in solution, so that they can be easily separated from other components in the mixture. Smaller oligos and other components remain in solution, while the DNA construct pellets at the bottom. Thus, determining the optimal concentration of the precipitant (PEG or ethanol) is required on a structure-by-structure basis to selectively separate the structure. DNA constructs that are comparable in size to their constituent oligos (such as the DNA tetrahedron made of merely 4 oligos) cannot be purified by such precipitating agents. The quality of DNA nanostructure purified via PEG is just as good as ultrafiltration techniques since larger MW DNA nanostructures are retained but smaller residual oligos are separated. For unmodified DNA constructs, PEG precipitation remains a superior method, as quantity purified is as high as 95%.[31] However, yield tends to trend downward for functionalized nanostructures, with an average yield of around 75%.[26] Surprisingly, no cytotoxic effects are noted in studies that subject *in vitro* or *in vivo* models to the PEG-purified DNA nanostructures, although residual PEG on the DNA nanostructures after precipitation is yet to be quantified.[5,33,34] Moreover, PEG precipitation is performed under high $Na^+$ concentration; to what extent does salt exchange take place when DNA nanostructure prepared in $Mg^{2+}$ is PEG purified is also unclear.

When DNA origami structures are applied to cellular applications, it is important to maintain the structural integrity under physiological conditions. With some of the more common purification methods, the functionality of these nanostructures in biological fluids is often hindered due to denaturation caused by physiological salt conditions as well as degradation by various nucleases.[35] To combat this, one of the most promising technique is oligolysine-PEG precipitation (K10PEG). With this purification method, the DNA backbone is coated with PEG (the same manner as PEG-precipitation), but additionally, there is a short lysine tail that protrudes to prevent degradation attacks by circulating nucleases.[36] This method has been shown to stabilize DNA origami nanostructures for over 48 h in harsh conditions.[36] This stability increase, as well as no detectable cellular toxicity, allows for nanostructures purified in this way to be used in a wide range of biomedical applications. It is unclear, though, whether precipitation-based purifications interfere with DNA nanostructure functionality when applied as photonic or plasmonic nanosystems since nano environments around optically active species greatly influence their photophysical properties. PEG precipitation can nevertheless be classified as a medium-quality technique (since higher MW byproducts are retained) producing a high quantity of nanostructure.

Its principles make this purification method ideal for biological applications, but its effectiveness in other disciplines requires further verification.

One other drawback of ultrafiltration and PEG precipitation is that their basis of centrifugation enhances aggregation and shear damage in samples. In the case of ultrafiltration, the DNA sample is eluted in lower than original starting volume by nature of the technique, whereas in PEG precipitation the sample is reconstituted after completely precipitating. Thus, in both approaches the centrifugation and change in sample concentration can worsen nanostructure dispersity. One can overcome the challenge of aggregation by storing the DNA nanostructure at lower salts and lyophilization. Prior to applying the DNA nanostructure, simply reconstituting the sample in water was shown to pose no aggregation issues.[30] Lyophilization, commonly utilized for the long-term storage of biomolecules, is a technique in which the sample is shock-frozen in liquid nitrogen and, in turn, subjected to sublimation under vacuum. This technique leaves behind solid components in a sample, including salts; thus, it is imperative that the initial buffer be of minimal salt concentration before subjecting a sample to this freeze-drying process (Figure 3A). Salt concentration is again dependent on nanostructure geometry; dense structures tend to require higher levels of salt for prolonged structural integrity.[30] It is hypothesized that the rapid exclusion of salt and EDTA during shock-freezing reduces the DNA nanostructure-to-nanostructure aggregation. After this initial lyophilization, samples can be resuspended in water (or buffer of choice), and a homogeneous sample would be achieved. DNA nanostructure conformation can be verified via microscopy, but the extent of structure preservation remains to be studied in detail. Though this is not a purification technique, it is mentioned as a means of improving the quality (even dispersion) of a purified sample after subjection to more common purification methods such as ultrafiltration and PEG precipitation.

One affinity-based technique is magnetic bead-based separation. The underlying concept for this technique lies within the favorable binding interaction between the protein streptavidin and its small molecular ligand biotin. Here, magnetic beads are coated in streptavidin (and are commercially available), and if a product of interest (DNA nanostructure, in our case) is labeled with a biotin tag, then, when mixed with streptavidin coated beads, the desired product will bind to the magnetic bead and be isolated from its other constituents in solution using a magnet. Magnetic bead-based separation is useful in targeted isolation of scaffold strands in enzymatic methods of synthesizing custom ssDNAs by using biotinylated primer strands (Figure 3B).[37,38] This method has been successful in purifying DNA constructs that have been functionalized with dyes/proteins/nanoparticles, with average yields within the range of 50–70%.[26] Herein, magnetic beads were combined with a biotin-labeled ssDNA and the DNA nanostructure was modified with a capture staple strand containing an extended complementary sequence. DNA nanostructures were captured by hybridization between the extended capture staple strand and DNA on the magnetic beads. After the residual solution was removed and the beads and DNA nanostructure mixture were reconstituted in fresh solution, the nanostructures could be released using DNA strand displacement. Suffice it to say that this technique should separate unfunctionalized DNA nanostructures from excess staples well too. Qualitatively, magnetic bead-based separation is

unique in that it eliminates impurities that do not bind to the biotin staples, so higher-order byproducts may get retained.

The selectivity of magnetic bead-based separation is strongly correlated to the number of biotin binding sites on the DNA nanostructure. As previously noted, the DNA origami assembly can yield impurities in which a structure is not completely formed and is missing one or more staples. To isolate structures with higher structural integrity (more fully formed), a sequential pull-down purification method using magnetic beads can be employed.[39] The effectiveness of this approach was showcased through the purification of linear origami superstructures using a two-sided pull-down reaction, as well as the purification of a T-shaped superstructure using a three-sided pull-down reaction (Figure 3C).[39] The baseline assumes that a pure superstructure will retain all the termini, and if each terminus of a structure is tagged with an anchor strand, then pure structures can be separated from impure ones (missing termini) by means of using a capture strand to sequentially retain desired components. The importance of performing multiple pull-downs relies upon the idea that some impure structures may retain certain anchor strands, but the likelihood of an impurity or partially formed structure will carry with it all of the possible anchor strands is nearly zero. It can be presumed that a pure/well-formed structure retains all anchor strands, and because of this, impure substructures can be eliminated in “rounds”, and the end result will be a purified origami solution. This analytical technique resulted in a purity of 93 ± 5% compared to the original solution as measured by TEM images.[39] Impurities left over in the solution were assumed to be excess release strands that were removed via PEG precipitation. TEM confirmed the removal of these slight impurities; however, the overall percentage of nanostructures that were left in the sample was reduced to 74 ± 3%.[39] These results suggest that the pull-down purification method is gentler on origami superstructures when compared to a more common technique such as PEG. This universal/versatile method can in theory be utilized in a variety of DNA nanotechnology applications due to its high level of purity. Scalability is also possible by proportionately adding more streptavidin-coated magnetic beads. Magnetic beads as an irreversible consumable needed for this technology is comparable to ultrafiltration columns in cost, but the method does require a more in-depth origami design, complexity of the purification steps, as well as a longer purification time, which need to be addressed before scalability becomes achievable.

A few other noteworthy purification techniques include size-exclusion chromatography (SEC),[27] ultracentrifugation,[40,41] ethanol precipitation,[32] capillary electrophoresis,[42] and dialysis.[43] Details of their efficacy are listed in Table 1. Individually, each of these aforementioned methods has a variable effect in achieving a pure DNA construct and is observed infrequently in the literature. More recent efforts have focused on two larger goals: one to scale up the production of DNA nanostructures and one to scale up the size of DNA nanostructures through multimeric assembly (see SI).

## CHARACTERIZATION OF DNA NANOSTRUCTURES

Characterization of DNA origami structures plays a crucial role in understanding their properties, assessing their quality, and guiding their application. Accurate and comprehensive characterization techniques enable researchers to validate the structural

integrity of DNA nanostructures and to estimate the size and shape of the formed product. There are many common characterization techniques that provide valuable information regarding DNA origami structure, but none are comprehensive; they are used in tandem to create a complete characterization data set. Because of this, expanding these methodologies to overcome certain limitations is important. Current characterization techniques as well as their respective advantages and disadvantages are summarized in Table 2. Below, we highlight some of the most-applied approaches.

Atomic force microscopy (AFM) is a single-molecule microscopy technique that provides valuable insight into the topography or surface of DNA nanostructures. AFM operates by scanning a cantilever with a sharp tip over the surface of a sample, and through that interaction, the deflection of light is recorded in order to give high-resolution images of the material. This technique is able to capture lateral details with a resolution ranging from 1 to 10 nm and a height resolution of 0.1 nm.[44] AFM offers many advantages, the most notable being that this technique requires minimal sample preparation and can be carried out under atmospheric conditions.[44] AFM was first developed to investigate the surface of insulators in 1986, but it was quickly adapted into the field of DNA nanotechnology.[24,45] Since then, AFM has proven to be a dominant tool for characterizing nanostructures of all geometries and is

presented in nearly every DNA nanostructure-related publication as evidence. AFM imaging is generally carried out through tapping mode on the instrument with the DNA nanostructure sample immersed in a compatible imaging solution. The sample is deposited on a mica substrate, a layered mineral chosen because of its smooth texture. DNA nanostructures can also be imaged when deposited on glass substrates.[46] In sample preparation, the top layer of the mica surface is removed with either Scotch tape or a razor blade; this will ensure a clean and even working surface that is suitable for nanoscale imaging.[47] Mica surfaces are negatively charged, and because of this, the surface generally must be flooded with divalent cations in order to facilitate the adsorption of the negatively charged DNA constructs.[47] Luckily, DNA nanostructures are prepared with cations such as $Mg^{2+}$ and $Na^{+}$, which facilitate their adsorption to the mica. Oftentimes, imaging buffer is supplemented with nickel chloride to increase adsorption.[46] The ideal concentration of DNA nanostructures should lie between 0.01 and 0.8 $\mu$g/mL depending on nanostructure size (higher concentration for smaller structures).[48] For DNA nanostructures that are 100 nm along one dimension, this translates to a 2–10 nM concentration. Samples that are imaged with too high of a concentration may exhibit aggregation, preventing accurate characterization of individual DNA nanostructure geometries. AFM provides qualitative surface information at a theoretical resolution of 1 nm. In practice, it is challenging to achieve highly precise imaging of DNA nanostructures at a resolution below 10 nm due to the softness of DNA as a material and the invasive nature of the AFM imaging cantilever. Precision can be enhanced by combinatorial imaging using AFM and super-resolution microscopy.[46] Nevertheless, AFM serves as the go-to technique to broadly determine the structural dispersity of DNA nanostructures at ~10 nm resolution. A small population (few hundred) of the DNA nanostructures is manually evaluated and binned into “well-formed” and “defective” conformations to estimate the assembly yield. Manual analysis through counting not only is tedious but can also inject bias into the analysis. Machine learning

tools are being developed to facilitate high-throughput quantitative evaluation of DNA nanostructures through AFM analysis (Figure 4A).[49]

Transmission electron microscopy (TEM) is an imaging technique that is based on the interaction between a high-energy electron beam and the sample. In traditional TEM, electrons are accelerated to high speeds and focused onto a sample deposited on a carbon grid substrate by using electromagnetic lenses. As these electrons pass through the sample, they interact with the sample and scatter; this scattering pattern is captured by a detector, and in turn, an image is generated that outlines the surface details of the sample. TEM was first developed in 1931 by Ruska, and its underlying principles have since been translated to the imaging of DNA nanostructures.[24,50] Typically, DNA constructs need to be stained using heavy atom salts such as uranyl formate or acetate in order to achieve a high-contrast image; the uranium ions in these salts interact with the negatively charged backbone of the DNA resulting in the formation of a high-density stain around the DNA nanostructure.[51] While uranyl salts are advantageous to contrast enhancement, it should also be noted that this staining process poses a high hazard risk level and is not easily permissible. Staining can introduce artifacts to the image when the sample is exposed to the electron beam for a long period of time.[52] Additionally, this heavy metal staining may cause some distortion or shrinkage of the sample, potentially affecting the accuracy of the depicted DNA nanostructures.[53] Alternative stains that are not as hazardous, such as the “UranyLess” stain, are available but have not gained sufficient traction in the community. TEM is crucial for various applications to obtain images of three-dimensional DNA structures in order to obtain an accurate understanding of their shape.[54,55] Imaging unstained DNA constructs in their native form (unstained) will allow for an accurate determination of nanostructure design, but this poses a significant challenge, as depositing DNA onto dry carbon membranes often results in poor contrast, and therefore a low-resolution image.[54,55] Perhaps if attention is pulled from the sample preparation and directed toward modifying the electron optics, a high-contrast image can be achieved without the use of heavy atom salts. In 2019, three in-focus phase contrast TEM techniques were developed, as shown in Figure 4B: sub-Angstrom low-voltage electron microscopy (SALVE), dark-field (DF) microscopy, and the use of a volta-potential phase plate (VPP).[55] SALVE uses a low-frequency electron beam (20 kV) which is beneficial for studying sensitive samples. Low-energy electrons are less penetrating than their high-energy counterparts, and because of that, higher contrast and resolution can be achieved when imaging thin samples (such as DNA nanostructures). Similarly, in using low-energy electrons for TEM imaging, electron scattering is minimized, resulting in clear, refined images. This technique is particularly applicable to DNA nanostructures that will ultimately be used in biomedical applications.[55] Despite the significant advancement made by this technique, SALVE microscopes are still very limited, encouraging researchers to find other ways to image DNA nanostructures in their native form. In contrast, DF microscopy tools are something that can easily be integrated into any traditional TEM. This technique provides the contrast necessary for DNA visualization at high voltages (300 kV) and works by using an aperture (circular disc with central opening) and positioning the scattering angle of the electron beam such that only scattered electrons can pass through its opening. Subsequently, these scattered electrons contribute to the formation of the image, leaving behind a dark background. This

contrast allows for the visualization of structures that would otherwise be hard to capture with traditional brightfield imaging. This would be the prevailing method when analyzing inorganic samples; diffracted beams are stronger for inorganic materials when compared to biomolecules, and because of this, only a portion of the refracted beams are necessary to form a high-contrast image.[55] However, in translating the technique to DNA nanostructures, DF microscopy has still proven to be efficient so long as the instrument is set to wide-field mode.[55] The third technique that can be utilized for the imaging of DNA constructs is by conducting TEM with the use of a volta-potential phase plate. The VPP is a specialized device made of a thin carbon film with a central opening. Once the electrons are inserted into the microscope, a voltage is applied, changing how the electrons behave as they pass through the opening. This applied current creates a phase shift in the incident electron beam, and this small variation is what allows for the creation of a more defined, high-resolution image.[55] The VPP setup is also something that can be added to a traditional transmission electron microscope, increasing the applicability of this technique to all researchers.

While AFM and TEM are suitable modes for assessing a singular active surface of a DNA construct, these characterization techniques are still lacking in providing a comprehensive 3D view of a structure in one image. Fluorescence microscopy is a technique that allows for the visualization of molecules at the nm resolution.[56] Typically, a sample is labeled with one or more fluorophores (or fluorescent dyes) at specific regions of interest, and as a result, the sample can be tracked via fluorescence microscopy. In relation to DNA origami constructs, this is done by simply replacing one of the outer staple strands with a dye-labeled staple strand.[57] Fluorescent-labeling is especially useful in biological applications; if a nanostructure is tagged with a fluorescent dye, movement of the structure can easily be tracked in a cell.[58] However, this technique would also be applicable to materials science and nanotechnology, as it could aid in manipulating nanoscale materials and measuring the physical distance between two labeled species.[54]

One example of high-resolution fluorescence imaging is DNA-based point accumulation for imaging on the nanoscale topography (DNA-PAINT). This characterization method is used in accompaniment with an inverted fluorescence microscope and allows for high spatial resolution and single-strand visibility with 5–10 nm resolution.[36,59] In tagging a nanostructure with two or more different fluorophores, DNA-PAINT can be used to show hybridization kinetics of two or more sides of a DNA origami structure at the same time. The technique is especially beneficial for biological applications, as here, it is necessary for DNA origami structures to be functionalized with fluorophores, or other imaging molecules, so that the target structure can be tracked in a biological system.[36] As previously noted, nanostructure integrity in physiological conditions can be improved using K10PEG coating[35] which could affect super-resolution fluorescence activity of any fluorophores labeling on the DNA nanostructure substrate. Interestingly, in a 2021 study, a DNA origami disk with a diameter of 57 nm was used to analyze how effectively the fluorophores could be visualized even with the addition of the K10PEG protective coating. Results showed that the coating did not impede visualization of the DNA nanostructure, and with the use of the DNA-PAINT technique, measurements could be taken along both the *x*- and *z*-axes simultaneously (Figure 4C).

Cryo-electron microscopy (Cryo-EM) is another imaging technique that is used to visualize molecules at near atomic resolution. It involves freezing a sample in a thin layer of vitreous ice to preserve its native state. This aids in reducing the presence of any unwanted artifacts that are caused by conventional sample preparation methods.[60] In Cryo-EM, an electron beam is used to capture two-dimensional projection images of the frozen sample at different angles, and from these, a three-dimensional reconstruction of the imaged material can be generated. This technique was developed in 1974 with the hope of being able to image biological specimens with all of their water preserved, and keeping it cold enough to prevent evaporation was the driving force.[60] That being said, Cryo-EM is an excellent characterization method for DNA nanostructures, as in many cases, geometry of the nanostructure determines function, and it is essential to ensure that the DNA construct has formed correctly.[61] When applying Cryo-EM to DNA nanostructures, this technique is mainly used for constructs that are developed with a biological application in mind, but it is certainly relevant for any downstream application.[62,63] It is as a structural validation technique for 3D wireframe structures designed using tools such as DAEDALUS and also to validate the hierarchical assembly of DNA polyhedra from smaller DNA tiles, both of which are challenging to visualize using AFM and TEM due to their 3D nature and lower DNA density, respectively.[64,65] As an additional example, researchers set a goal of inserting a DNA origami nanostructure into a simian virus 40 capsid (SV40). This viral capsid has proven to be a promising biomaterial, as it has been used in various medical applications.[63,66,67] Negative stain TEM was used as a first assessment to determine whether or not the origami nanostructure had been completely coated by the capsid protein or if these two constituents remained as stand-alone products. Results showed that there were no origami structures that were partially coated.[63] The lack of intermediates indicated strong cooperativity in the assembly process, but Cryo-EM was utilized in order to achieve a complete 3D rendering of the sample and confirm this preliminary analysis. This technique has seen remarkable progress in regard to the level of detail that it provides,[62] but its availability is limited due to cost and the sophisticated expertise needed. These cutting-edge microscopes are difficult to acquire, operate, and maintain, which poses challenges for researchers in resource-constrained environments. Therefore, alternative techniques are needed that are more commonly available at our disposal.

Small-angle X-ray scattering (SAXS) is a powerful characterization technique in which a sample is exposed to X-rays at a small angle (typically 0.1–5°),[68] and the resulting diffraction is measured and analyzed to give insight regarding the size, shape, and overall organization of the sample, in this case, DNA nanostructures. SAXS is able to deliver structural information for molecules ranging between 1 and 200 nm in size, which is a common dimension for DNA constructs. Commonly, this technique is employed only sporadically to confirm a successful assembly of a DNA origami structure. However, recently, SAXS has been used to monitor folding and unfolding of DNA constructs as a function of temperature.[69] Additionally, it is possible to observe and quantify the electrostatic expansion (with sub-Å precision) between DNA helices as a function of decreasing salt concentrations (Figure 5).[69] In another application, a DNA origami switch was able to change conformations (open/closed) with the addition of $MgCl_2$, and the rate at which this happens was able to be determined using time-resolved SAXS.[70,71]

This technique has also shown success in determining the heterogeneity of DNA origami mixtures. DNA nanotubes composed of multiple subunits of set length were analyzed simultaneously using SAXS, and based on the output, the DNA nanotubes were able to be successfully differentiated and quantified by size.[72] Using SAXS for this purpose offers a groundbreaking level of detail, allowing researchers to explore the limitations of their nanostructures under different conditions. In shedding light on its stability and dynamics, an ideal environment can be achieved, leading to reliable and accurate results for downstream applications.

Aside from each of these common characterization techniques, there are some notable secondary methodologies that allow for the characterization of DNA structures but lack a direct visualization component. Dynamic light scattering (DLS),[73] UV-absorbance, and AGE (as discussed previously)[54] are all valid ways of obtaining preliminary data regarding assembly efficiency. However, each of these techniques is often rather vague in the level of detail that they are able to provide, so because of this, they are rarely used as a standalone means of characterization. For this reason, advantages and disadvantages of each of the techniques are outlined in Table 2, but specifics of each technique will not be expanded upon.

## CONCLUSION AND FUTURE OUTLOOK

The field of DNA nanotechnology has a variety of applications, as highlighted in the introduction, but as researchers continue to refine and expand upon these, a comprehensive evaluation of nanostructure performance is yet to be achieved. As analytical techniques are applied and refined to cater to the needs of different applications, the scientific community could benefit from identifying standardized methods that maximize the yield and integrity of the structures. Overall cost of purification could be reduced by finding ways to recycle the constituents. Magnetic bead-based separation of formed DNA nanostructures from partially formed (through multistep bead-pulldown) and excess raw ingredients gives high purity and selectivity. However, the costs of the magnetic beads and low recycling capabilities prevent its widespread application. Similarly, microscopy techniques remain the dominant characterization techniques, but state-of-the-art AFM/EMs (and training to use them) are still few and far between.

A few techniques have been explored in a limited range for analyzing DNA nanostructures, namely, mass spectrometry-based tools[74] and capillary electrophoresis.[42] The former, in the MALDI-TOF format, currently falls short in the molecular weights of biomolecules that can be characterized (<300 kDa), and advancements in the technology are needed. The latter could offer the resolution required to differentiate DNA nanostructures with “a few” missing staple strands and serve well, albeit on a smaller laboratory scale.

With the rapid expansion of machine learning capabilities, advancements should focus on design tools that leverage the current database of fully characterized and published DNA nanostructures (nanobase.org) to design new architectures catering to different applications. Over the last two decades, hundreds of thousands of staples have likely been synthesized and acquired around the world in quantities that often outlast the length of a project (or

a PhD thesis). Reverse engineering a DNA nanostructure from a given set of staples is now possible;[75] perhaps these existing staples can be repurposed and remixed to create new viable architectures. Recycling the same scaffold into forming a new shape was recently shown by Pfeifer et al.[76] Such dynamism has the capability to make DNA nanotechnology an even "greener" technology while also be leveraged for multiplexed sensing and cellular applications.

## Supplementary Material

Refer to Web version on PubMed Central for supplementary material.

## ACKNOWLEDGMENTS

All the authors were supported by the National Institute of Biomedical Imaging and Bioengineering of the National Institutes of Health under Award Number R00EB030013. The content is solely the responsibility of the authors and does not necessarily represent the official views of the National Institutes of Health.

## Biographies

***Kayla Neyra*** is a PhD student in the Department of Chemistry at Case Western Reserve University. Her research is focused on using DNA origami as a platform for gene-delivery and gene-editing applications.

***Heather R. Everson*** is a PhD student in the Department of Chemistry at Case Western Reserve University. Her thesis project focuses on promoting endosomal escape via substituting magnesium with calcium as a DNA-origami counterion.

***Divita Mathur*** is an assistant professor in Chemistry at Case Western Reserve University where her group is pursuing the structural role of synthetic DNA in molecular organization and delivery systems. She teaches quantitative analytical chemistry and bioconjugate chemistry.

## REFERENCES

(1). Sachenbacher K; Khoshouei A; Honemann MN; Engelen W; Feigl E; Dietz H ACS Nano 2023, 17 (10), 9014–9024. [PubMed: 37159224]

(2). Chandrasekaran AR; Rusling DA Nucleic Acids Res. 2018, 46 (3), 1021–1037. From NLM [PubMed: 29228337]

(3). Ng C; Samanta A; Mandrup OA; Tsang E; Youssef S; Klausen LH; Dong M; Nijenhuis MAD; Gothelf KV Adv. Mater. 2023, 35 (40), No. e2302497. From NLM [PubMed: 37311656]

(4). Madsen M; Gothelf KV Chem. Rev. 2019, 119 (10), 6384–6458. [PubMed: 30714731]

(5). Lucas CR; Halley PD; Chowdury AA; Harrington BK; Beaver L; Lapalombella R; Johnson AJ; Hertlein EK; Phelps MA; Byrd JC; et al. Small 2022, 18 (26), No. e2108063. [PubMed: 35633287]

(6). Knappe GA; Wamhoff EC; Bathe M Nat. Rev. Mater. 2023, 8 (2), 123–138. [PubMed: 37206669]

(7). Song L; Jiang Q; Wang ZG; Ding B ChemNanoMat 2017, 3 (10), 713–724.

(8). Mathur D; Medintz IL Adv. Healthc Mater. 2019, 8 (9), No. e1801546. [PubMed: 30843670]

(9). Pettersen EF; Goddard TD; Huang CC; Couch GS; Greenblatt DM; Meng EC; Ferrin TE J. Comput. Chem. 2004, 25 (13), 1605–12. [PubMed: 15264254]

(10). Jiao Y; Shang Y; Li N; Ding B iScience 2022, 25 (4), No. 104018. [PubMed: 35313688]

(11). Zhang Q; Jiang Q; Li N; Dai L; Liu Q; Song L; Wang J; Li Y; Tian J; Ding B; et al. ACS Nano 2014, 8 (7), 6633–6643. [PubMed: 24963790]

(12). Keller A; Linko V Angew. Chem., Int. Ed. Engl. 2020, 59 (37), 15818–15833. [PubMed: 32112664]

(13). Ijas H; Shen B; Heuer-Jungemann A; Keller A; Kostiainen MA; Liedl T; Ihalainen JA; Linko V Nucleic Acids Res. 2021, 49 (6), 3048–3062. From NLM [PubMed: 33660776]

(14). Liang H; Zhang XB; Lv Y; Gong L; Wang R; Zhu X; Yang R; Tan W Acc. Chem. Res. 2014, 47 (6), 1891–1901. [PubMed: 24780000]

(15). Wang WX; Douglas TR; Zhang H; Bhattacharya A; Rothenbroker M; Tang W; Sun Y; Jia Z; Muffat J; Li Y; et al. Nat. Nanotechnol 2024, 19 (1), 58–69. [PubMed: 37500778]

(16). Yang Q; Chang X; Lee JY; Olivera TR; Saji M; Wisniewski H; Kim S; Zhang F ACS Appl. Bio Mater. 2022, 5, 4652. From NLM Publisher

(17). Wang S; Zhou Z; Ma N; Yang S; Li K; Teng C; Ke Y; Tian Y Sensors (Basel) 2020, 20 (23), 6899. [PubMed: 33287133]

(18). Li S; Shi B; He D; Zhou H; Gao ZJ Hazard Mater. 2023, 458, No. 131874.

(19). Kuzyk A; Jungmann R; Acuna GP; Liu N ACS Photonics 2018, 5 (4), 1151–1163. [PubMed: 30271812]

(20). Mathur D; Diaz SA; Hildebrandt N; Pensack RD; Yurke B; Biaggne A; Li L; Melinger JS; Ancona MG; Knowlton WB; et al. Chem. Soc. Rev. 2023, 52 (22), 7848–7948. [PubMed: 37872857]

(21). Hao Y; Li Q; Fan C; Wang F Small Structures 2021, 2 (2), No. 2000046.

(22). Fan S; Wang D; Cheng J; Liu Y; Luo T; Cui D; Ke Y; Song J Angew. Chem., Int. Ed. Engl. 2020, 59 (31), 12991–12997. [PubMed: 32304157]

(23). Fan C; Li Q Small 2019, 15 (26), No. e1902586. [PubMed: 31355531]

(24). Rothemund PW Nature 2006, 440 (7082), 297–302. [PubMed: 16541064]

(25). Perry-O'Keefe H; Yao XW; Coull JM; Fuchs M; Egholm M Proc. Natl. Acad. Sci. U. S. A. 1996, 93 (25), 14670–14675. From NLM [PubMed: 8962112]

(26). Shaw A; Benson E; Hogberg B ACS Nano 2015, 9 (5), 4968–4975. [PubMed: 25965916]

(27). Wagenbauer KF; Engelhardt FAS; Stahl E; Hechtl VK; Stommer P; Seebacher F; Meregalli L; Ketterer P; Gerling T; Dietz H Chembiochem 2017, 18 (19), 1873–1885. [PubMed: 28714559]

(28). Hall AC bioRxiv 2020, No. 568253.

(29). Douglas SM; Marblestone AH; Teerapittayanon S; Vazquez A; Church GM; Shih WM Nucleic Acids Res. 2009, 37 (15), 5001–5006. [PubMed: 19531737]

(30). Baptist AV; Heuer-Jungemann A ACS Omega 2023, 8 (20), 18225–18233. [PubMed: 37251192]

(31). Stahl E; Martin TG; Praetorius F; Dietz H Angew. Chem., Int. Ed. Engl. 2014, 53 (47), 12735–12740. From NLM [PubMed: 25346175]

(32). Lei Y; Mei Z; Chen Y; Deng N; Li Y ChemNanoMat 2022, 8 (7), No. e202200161.

(33). Kretzmann JA; Liedl A; Monferrer A; Mykhailiuk V; Beerkens S; Dietz H Nat. Commun. 2023, 14 (1), 1017. [PubMed: 36823187]

(34). Wu X; Yang C; Wang H; Lu X; Shang Y; Liu Q; Fan J; Liu J; Ding BJ Am. Chem. Soc. 2023, 145 (16), 9343–9353.

(35). Ponnuswamy N; Bastings MMC; Nathwani B; Ryu JH; Chou LYT; Vinther M; Li WA; Anastassacos FM; Mooney DJ; Shih WM Nat. Commun. 2017, 8, 15654. [PubMed: 28561045]

(36). Eklund AS; Comberlato A; Parish IA; Jungmann R; Bastings MMC ACS Nano 2021, 15 (11), 17668–17677. [PubMed: 34613711]

(37). Silva-Santos AR; Oliveira-Silva R; Sousa Rosa S; Paulo PMR; Prazeres DMF ACS Applied Nano Materials 2021, 4 (12), 14169–14177.

(38). Yuce M; Kurt H; Budak H Anal. Methods 2014, 6 (2), 548–557.

(39). Ye J; Teske J; Kemper U; Seidel R Small 2021, 17 (17), No. e2007218. [PubMed: 33728738]

(40). Lin C; Perrault SD; Kwak M; Graf F; Shih WM Nucleic Acids Res. 2013, 41 (2), No. e40. (acccessed 8/4/2023) [PubMed: 23155067]

(41). Ko SH; Vargas-Lara F; Patrone PN; Stavis SM; Starr FW; Douglas JF; Liddle JA Soft Matter 2014, 10 (37), 7370–7378. [PubMed: 25080973]

(42). Hui J; Majikes JM; Riley KR Anal. Chem. 2023, 95 (51), 18783–18792. [PubMed: 38088564]

(43). Jungmann R; Liedl T; Sobey TL; Shih W; Simmel FC J. Am. Chem. Soc. 2008, 130 (31), 10062–10063. [PubMed: 18613687]

(44). Bald I; Keller A Molecules 2014, 19 (9), 13803–13823. [PubMed: 25191873]

(45). Binnig G; Quate CF; Gerber C Phys. Rev. Lett. 1986, 56 (9), 930–933. [PubMed: 10033323]

(46). Green CM; Schutt K; Morris N; Zadegan RM; Hughes WL; Kuang W; Graugnard E Nanoscale 2017, 9 (29), 10205–10211. [PubMed: 28489095]

(47). Lyubchenko YL; Shlyakhtenko LS; Ando T Methods 2011, 54 (2), 274–283. [PubMed: 21310240]

(48). Lyubchenko YL; Gall AA; Shlyakhtenko LS Methods Mol. Biol. 2014, 1117, 367–384. [PubMed: 24357372]

(49). Chiriboga M; Green CM; Hastman DA; Mathur D; Wei Q; Diaz SA; Medintz IL; Veneziano R Sci. Rep 2022, 12 (1), No. 3871. [PubMed: 35264624]

(50). Ruska E Biosci Rep 1987, 7 (8), 607–629. [PubMed: 3322421]

(51). Harris JR; De Carlo S Methods Mol. Biol. 2014, 1117, 215–258. [PubMed: 24357366]

(52). Bertosin E; Stommer P; Feigl E; Wenig M; Honemann MN; Dietz H ACS Nano 2021, 15 (6), 9391–9403. [PubMed: 33724780]

(53). Gallagher JR; Kim AJ; Gulati NM; Harris AK Curr. Protoc Microbiol 2019, 54 (1), No. e90. [PubMed: 31518065]

(54). Dey S; Fan C; Gothelf KV; Li J; Lin C; Liu L; Liu N; Nijenhuis MAD; Sacca B; Simmel FC; et al. Nature Reviews Methods Primers 2021, 1 (1), 13.

(55). Kabiri Y; Ravelli RBG; Lehnert T; Qi H; Katan AJ; Roest N; Kaiser U; Dekker C; Peters PJ; Zandbergen H Sci. Rep 2019, 9 (1), 7218. [PubMed: 31076614]

(56). Steinhauer C; Jungmann R; Sobey TL; Simmel FC; Tinnefeld P Angew. Chem., Int. Ed. Engl. 2009, 48 (47), 8870–8873. [PubMed: 19830751]

(57). Schmied JJ; Raab M; Forthmann C; Pibiri E; Wunsch B; Dammeyer T; Tinnefeld P Nat. Protoc 2014, 9 (6), 1367–1391. [PubMed: 24833175]

(58). Mathur D; Rogers KE; Díaz SA; Muroski ME; Klein WP; Nag OK; Lee K; Field LD; Delehanty JB; Medintz IL Nano Lett. 2022, 22 (12), 5037–5045. [PubMed: 35580267]

(59). Dai M Methods Mol. Biol. 2017, 1500, 185–202. From NLM [PubMed: 27813009]

(60). Dubochet JJ Microsc 2012, 245 (3), 221–224.

(61). Ahmad K; Javed A; Lanphere C; Coveney PV; Orlova EV; Howorka S Nat. Commun. 2023, 14 (1), 3630. [PubMed: 37336895]

(62). Bai XC; Martin TG; Scheres SH; Dietz H Proc. Natl. Acad. Sci. U. S. A. 2012, 109 (49), 20012–20017. [PubMed: 23169645]

(63). Kopatz I; Zalk R; Levi-Kalisman Y; Zlotkin-Rivkin E; Frank GA; Kler S Nanoscale 2019, 11 (21), 10160–10166. [PubMed: 30994643]

(64). He Y; Ye T; Su M; Zhang C; Ribbe AE; Jiang W; Mao C Nature 2008, 452 (7184), 198–201. [PubMed: 18337818]

(65). Veneziano R; Ratanalert S; Zhang K; Zhang F; Yan H; Chiu W; Bathe M Science 2016, 352 (6293), 1534. [PubMed: 27229143]

(66). Seitz I; Saarinen S; Kumpula EP; McNeale D; Anaya-Plaza E; Lampinen V; Hytonen VP; Sainsbury F; Cornelissen J; Linko V; et al. Nat. Nanotechnol 2023, 18 (10), 1205–1212. [PubMed: 37460794]

(67). Kler S; Zalk R; Upcher A; Kopatz I Nanoscale 2022, 14 (32), 11535–11542. [PubMed: 35861608]

(68). Liu L; Boldon L; Urquhart M; Wang X J. Vis Exp 2013, No. 71, e4160 From NLM DOI: 10.3791/4160.

(69). Fischer S; Hartl C; Frank K; Radler JO; Liedl T; Nickel B Nano Lett. 2016, 16 (7), 4282–4287. [PubMed: 27184452]

(70). Bruetzel LK; Gerling T; Sedlak SM; Walker PU; Zheng W; Dietz H; Lipfert J Nano Lett. 2016, 16 (8), 4871–4879. [PubMed: 27356232]

(71). Bruetzel LK; Walker PU; Gerling T; Dietz H; Lipfert J Nano Lett. 2018, 18 (4), 2672–2676. [PubMed: 29554806]

(72). Zhu B; Guo J; Zhang L; Pan M; Jing X; Wang L; Liu X; Zuo X Chembiochem 2019, 20 (12), 1508–1513. [PubMed: 30702811]

(73). Yuan W; Dong G-Z; Ning H; Guan X-X; Cheng J-F; Shi Z-W; Du X-J; Meng S-W; Liu D-S; Dong Y-C Chin. Chem. Lett. 2024, 35 (3), No. 108384.

(74). van Dyck JF; Burns JR; Le Huray KIP; Konijnenberg A; Howorka S; Sobott F Nat. Commun. 2022, 13 (1), 3610. [PubMed: 35750666]

(75). Shirt-Ediss B; Connolly J; Elezgaray J; Torelli E; Navarro SA; Bacardit J; Krasnogor N Comput. Struct Biotechnol J. 2023, 21, 3615–3626. [PubMed: 37520280]

(76). Pfeifer WG; Huang CM; Poirier MG; Arya G; Castro CE Sci. Adv. 2023, 9 (30), No. eadi0697. [PubMed: 37494445]

(77). Mathur D; Medintz IL Anal. Chem. 2017, 89 (5), 2646–2663. [PubMed: 28207239]

(78). Oktay E; Bush J; Vargas M; Scarton DV; O'Shea B; Hartman A; Green CM; Neyra K; Gomes CM; Medintz IL; et al. ACS Appl. Mater. Interfaces 2023, 15 (23), 27759–27773. [PubMed: 37267624]

(79). Kuzuya A; Sakai Y; Yamazaki T; Xu Y; Komiyama M Nat. Commun. 2011, 2 (1), 449. [PubMed: 21863016]

(80). Prinz J; Heck C; Ellerik L; Merk V; Bald I Nanoscale 2016, 8 (10), 5612–5620. [PubMed: 26892770]

(81). Timm C; Niemeyer CM Angew. Chem., Int. Ed. Engl. 2015, 54 (23), 6745–6750. [PubMed: 25919336]

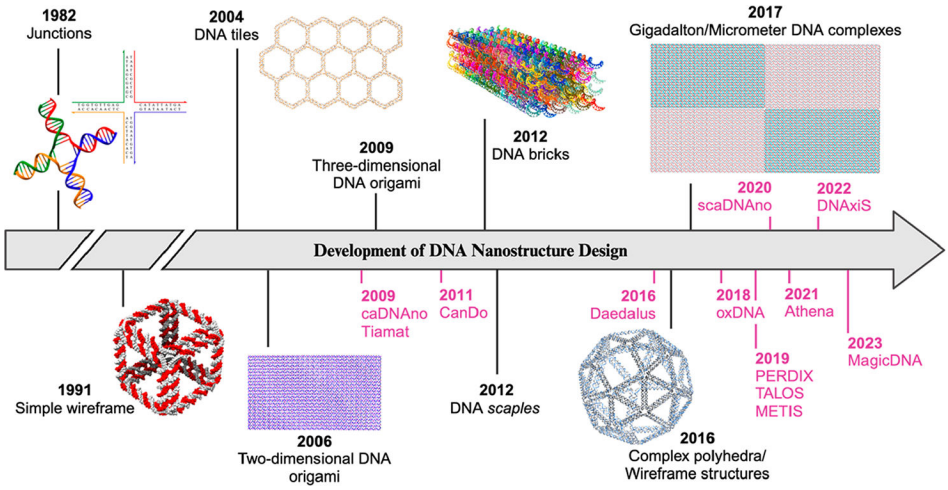


**Figure 1.**

Representative self-assembling DNA nanostructures arranged in order of design complexity over time. Oftentimes, challenges in purification and characterization are not directly correlated to the structural complexity, making it necessary to optimize DNA nanostructure analytical chemistry on a case-by-case basis. From left to right: Holliday junction (9.5 nm), simple wireframe (edge length of 16 nm), hexagonal DNA tiles (25 nm diameter per tile), 2D DNA origami rectangle (98 nm wide), DNA brick (length 40 nm), snubcube polyhedral structure (edge length 20 nm), and multimeric DNA complex (>200 nm). Structural depiction is representative of the geometric advancements made in that time, but they do not necessarily correlate to the timeline in which these specific designs were published. All structural designs were recreated using UCSF Chimera.[9] Figure created with BioRender.com.

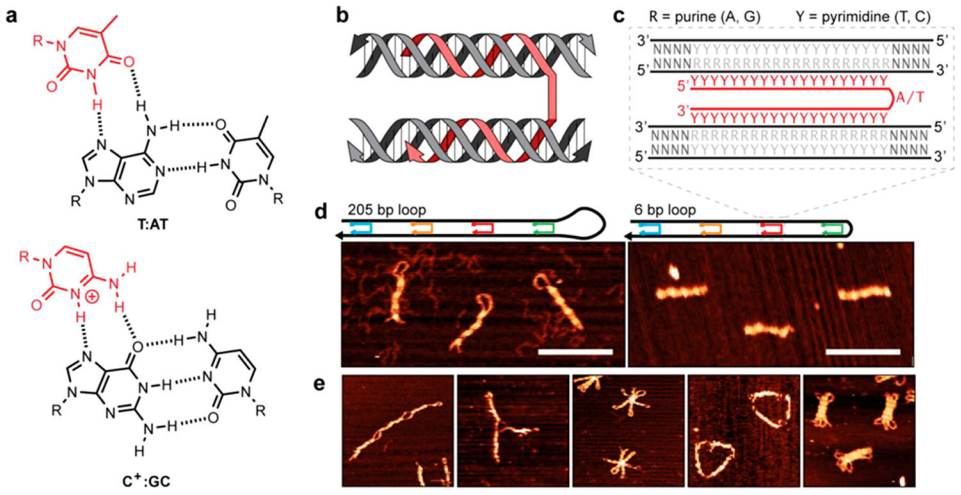


**Figure 2.**

Fundamentals behind triple-helix based DNA origami paradigm. (A) Hoogsteen (depicted by dashed bonds between bases in red and black) and Watson–Crick–Franklin (dashed lines between bases in black only) base pairing rules that enable DNA triple helix assembly. (B) Crossover schematic in a DNA triple helix assembly between two gray and 1 orange-red strand. (C) Sequence-design in triple helix assembly requires pyramidine-rich domains to form hydrogen bonds with a purine-rich track on the existing duplex. (D) Representative "chain" structures and (E) higher-order DNA nanostructures prepared using triple helix assembly. Scale bar = 100 nm. Reprinted with permission from ref 3. Copyright, 2023, John Wiley & Sons.

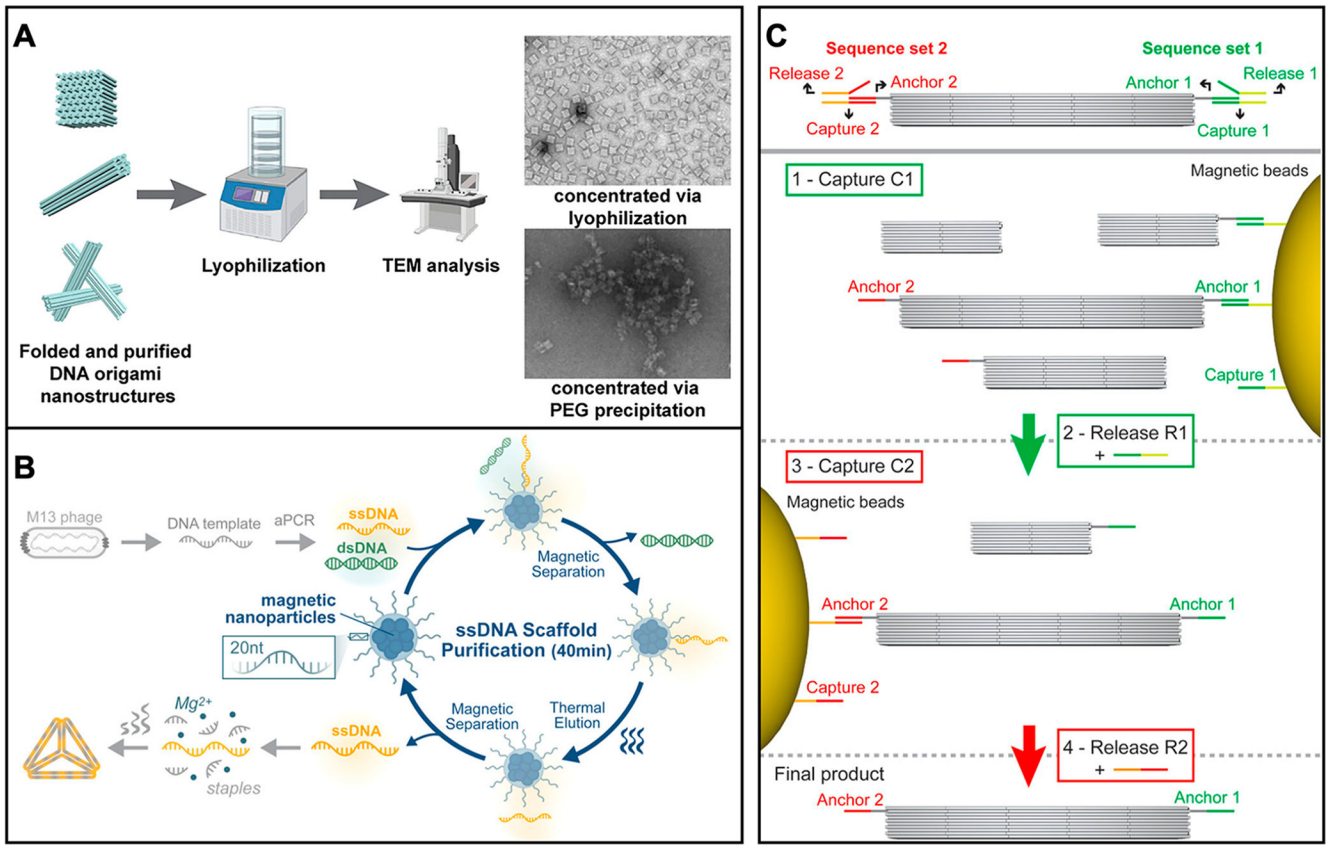


**Figure 3.**

Emerging purification techniques in DNA nanostructure analysis. (A) TEM image comparison for DNA origami nanostructures purified and concentrated via lyophilization and PEG precipitation.[30] (B) Schematic representative of how to isolate single-stranded scaffold DNA from a double-stranded DNA template using magnetic bead separation.[37] (C) Capture and release method for purification of DNA origami structures using functionalized magnetic beads. Reproduced with permission from ref 39. Copyright 2021 Wiley & Sons.

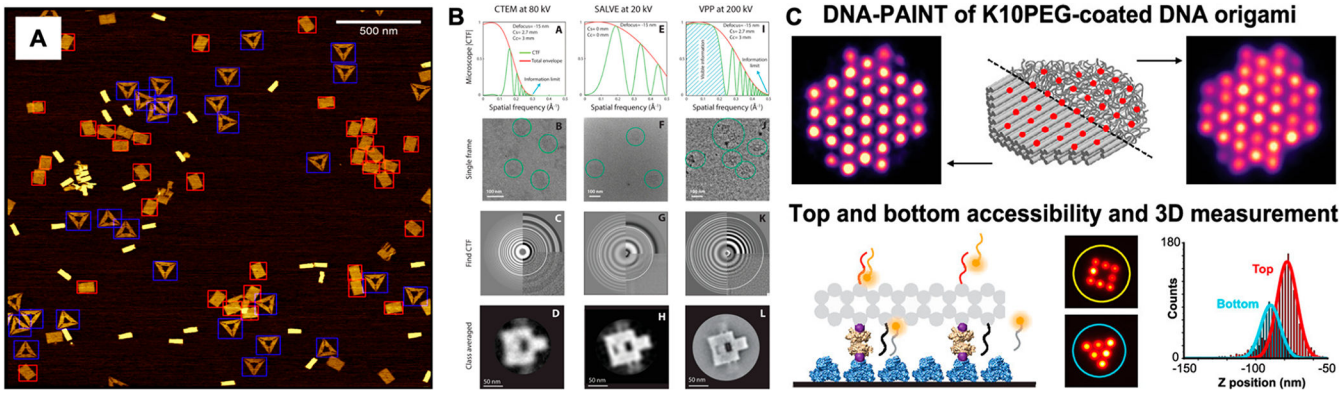


**Figure 4.**

Emerging microscopy characterization tools for DNA origami nanostructures. (A) Machine-learning enabled high-throughput analysis of a heterogeneous mix of DNA origami structures comprised of triangle, rectangle, and “imposter” DNA cylinders. The YOLO-v5 trained neural network successfully identified the triangles (blue boxes) and rectangles (red boxes) and dismisses the cylinders.[49] (B) Imaging of unstained DNA origami nanoplates on commercial carbon films. Column (A–D) shows results of 80 kV conventional TEM; column (E–H) shows result for 20 kV SALVE microscopy; column (I–L) shows result for VPP at 200 kV.[55] (C) Top: DNA origami disk with corresponding fluorescence microscopy images with (right) and without (left) a K10PEG coating. Bottom: Depiction of DNA origami disk binding to BSA-biotin-neutravidin slide accompanied by corresponding microscopy images of the top (square) and bottom (triangle) of the origami nanostructure. Analysis of the zposition is also available to give the height dimension.[36]

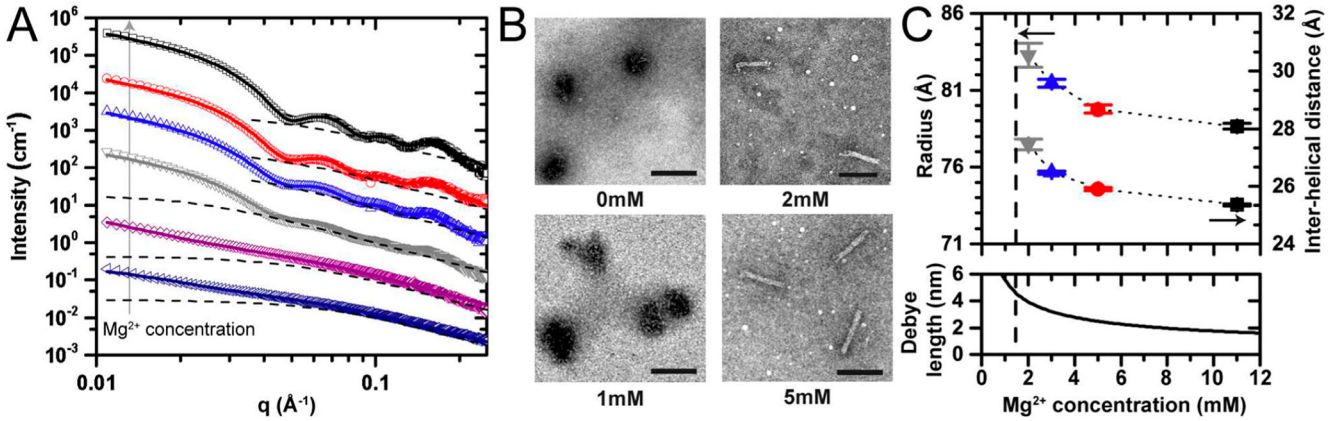


**Figure 5.**

Small-angle X-ray scattering (SAXS) characterization of DNA nanostructures. (A) SAXS scattering curves of a 24 helix-bundle in buffers with varying concentrations of $MgCl_2$. (B) TEM images for the 24 helix-bundle under various $MgCl_2$ concentrations. (C) Radii and Debye lengths for 24hb; concentrations of $MgCl_2$ correspond with data in A.[69]

**Table 1.**

Most Applied Techniques for DNA Nanostructure Purification

| Technique | Description | Example DNA str. (size) | Yield/ Efficiency | Pros | Cons | Reference |
|---|---|---|---|---|---|---|
| Agarose Gel Electrophoresis (AGE) | quick analysis of structure assembly, does not provide in-depth information at nucleotide level | geometry independent; no limitation | <30% | inexpensive | ~4 h; low recovery from extraction | 27 |
| Ultrafiltration | centrifuge filtration columns; vary in molecular weight cut off (MWCO) | 6hb (80 nm length); 18hb (13 nm × 138 nm); pentagonal bipyramid (18 nm edge) | 20–80% | <30 min; high yield for wireframe structures | low yield for dense structures; structures must be >30 kDa | 26, 77, 78 |
| PEG-precipitation | selectively pellets DNA aggregates so contaminants can be removed | geometry independent; no limitation | ~90% | consistent results; no toxicity for in vivo studies | >24 h; introduces residual PEG molecules to sample | 27, 31 |
| Magnetic Bead Separation | “tagged” constituents can be selectively isolated from rest of sample | geometry independent; no limitation | 30–70% | <1 h; no size limitation | expensive, as beads cannot be reused | 26, 77 |
| Size-Exclusion Chromatography (SEC) | Separates components by size, large molecules elute first | 3D nanostructures recommended; hexagonal 72hb *(assembles into higher order strs.)* | 70–90% | no volume limitation | ~3 h | 27 |
| Dialysis | diffusion of impurities through MWCO membranes | 2D: tile (100 nm x 70 nm); 3D: 6hb (410 nm length) | 70% | wide range MWCO | overnight; requires large sample volume; large contaminants remain | 43 |
| Ultracentrifugation | separates constituents based on density | 3D nanostructures; increased efficiency with large structures | 40–90% | 1 h; scalable | introduces new buffer | 40, 41 |
| Ethanol Precipitation | selectively pellets DNA aggregates so contaminants can be removed | 2D nanostructures; tile (100 nm × 70 nm); triangle (116 nm edge) | ~90% | inexpensive | variable efficiency depending on structure geometry | 32 |

**Table 2.**

Most Applied Techniques for DNA Nanostructure Characterization

| Technique | Advantages/Disadvantages | Cost/accessibility of technique | Complexity of technique | Common Application | References |
|---|---|---|---|---|---|
| Atomic Force Microscopy (AFM) | Cannot provide structural info on molecular level | Generally, as a core facility instrument | Expert | Multidisciplinary | 44, 79 |
| Transmission Electron Microscopy (TEM) | Cannot provide structural info on molecular level | Mostly a core facility instrument | Expert | Multidisciplinary | 54 |
| Fluorescence Microscopy | Constructs must be labeled with dyes; requires high sample concentration and large volume | Core facility/specialized lab instrumentation needed | Intermediate | Incorporation into biological samples | 54, 57 |
| Cryo-EM | Requires high sample concentration | Mostly a core facility instrument | Expert | Biomedical | 30, 60 |
| Small-Angle X-ray Scattering (SAXS) | Estimates dimensions for molecules between 1 and 200 nm; requires high sample concentration | Mostly a core facility instrument | Expert | Multidisciplinary | 30 |
| Dynamic Light Scattering (DLS) | Estimate dimensions of structure; requires high sample concentration and large volume | Specialized accessible lab instrumentation needed | Beginner | Mainly used for bare origami structures | 73 |
| UV—vis Absorbance | Estimates sample concentration, but requires purified DNA sample for accuracy; gives insight into potential sample contamination; advantageous for quantifying DNA structures with attached fluorophores | Commonly accessible instrumentation needed | Beginner | Multidisciplinary | 80, 81 |
| Agarose Gel Electrophoresis | Estimates assembly yield and efficiency | Commonly accessible instrumentation needed | Beginner | Multidisciplinary | 54 |